# FORMATION DRY-OUT FROM $CO_2$ INJECTION INTO SALINE AQUIFERS. PART 2, ANALYTICAL MODEL FOR SALT PRECIPITATION

Karsten Pruess

Earth Sciences Division, Lawrence Berkeley National Laboratory
University of California, Berkeley, CA 94720

**Abstract**

From a mass balance for water dissolved into the flowing $CO_2$ stream, and a consideration of saturation profiles from the Buckley-Leverett (1942) fractional flow theory, we derive an equation that directly relates gas saturation $S_{g,d}$ at the dry-out front to temperature, pressure and salinity dependence of fluid properties. The equation is easily solved by iteration or interpolation. From gas saturation at the front we derive the average gas saturation in the dry-out region, from which we obtain the "solid saturation" $S_S$, i.e., the fraction of pore space filled with solid precipitate. Values of $S_S$ derived from this theory show excellent agreement with numerical simulations presented in the preceding companion paper ("Part 1"). Thus, from relative permeabilities and fluid properties at *in situ* conditions prior to $CO_2$ injection, it is possible to directly make an accurate estimate of solids precipitation, without having to perform a numerical simulation of the injection process.

## 1. Introduction

This is Part 2 of a two-paper series addressing issues of formation dry-out and solids precipitation during $CO_2$ injection. The companion paper ("Part 1") presented numerical simulations of $CO_2$ injection in 1-D radial geometry along with arguments based on the similarity property of the problem to establish that solid saturation in the dry-out region is a constant, independent of space and time. This paper develops an analytical model based on water mass balance and fractional flow theory (Buckley and Leverett, 1942; Willhite, 1986) to directly calculate the solid saturation in the dry-out region. The applicability of our model is limited to conditions for which a similarity solution holds: constant rate of $CO_2$ injection into 1-D linear or radial flow geometry in a homogeneous medium with uniform initial conditions. As an additional

approximation, we need to neglect capillary pressure effects, in order to be able to invoke results from fractional flow theory.

Recent related work includes Nordbotten and Celia (2006), who considered injection of $CO_2$ in a confined aquifer in radial symmetry. They developed a vertically-averaged model that includes partitioning of $H_2O$ and $CO_2$ components between the aqueous and $CO_2$-rich phases, and formulated equations for the two-phase and dry-out fronts in terms of a similarity variable. Noh et al. (2007) used fractional flow theory to consider displacement of water by $CO_2$ with allowance for limited interphase mass transfer ("semimiscible displacement"). They also considered the propagation of dissolution fronts when aqueous $CO_2$ dissolves minerals such as calcite. The aforementioned studies did not address the potential for solids precipitation when dry-out occurs for an aqueous phase that includes dissolved solids, which is the main focus of this paper.

The organization of the paper is as follows. Sec. 2 presents development of the analytical model for solids precipitation. This is followed by illustrative solutions for a variety of problem parameters. Predictions from the analytical model are compared with detailed numerical simulations of $CO_2$ injection, using the general-purpose multiphase flow simulator TOUGH2 (Pruess, 2004), augmented with a fluid property module called ECO2N for mixtures of $H_2O$, $CO_2$, and NaCl (Pruess and Spycher, 2007). Some results from fractional flow theory that are used in our treatment are given in the Appendix.

## 2. Analytical Estimation of Salt Precipitation During Dry-Out

Injection of dry, supercritical $CO_2$ will give rise to immiscible displacement of resident aqueous phase, as well as inducing dissolution (evaporation) of water into the flowing $CO_2$ stream. In one space dimension, the process will be marked by two fronts, (1) the leading edge of two-phase conditions, or "displacement front," at distance $x_f$, and (2) a dry-out front at distance $x_d < x_f$ (see Fig. 1) When $CO_2$ is injected into saline water, formation dry-out will be accompanied by precipitation of solids, which will reduce porosity, permeability, and injectivity. We aim to estimate the fraction of pore space in the dry-out region that will be occupied by solid salt. In analogy to pore occupancy by multiple fluid phases, we term the fraction of pore space

occupied by solid precipitate the "solid saturation" $S_S$. Solid mass per unit formation volume is given by $m_s = \phi S_S \rho_s$, where $\phi$ is porosity, and $\rho_s$ is the density of the solid precipitate.

<Fig. 1 here>

The preceding companion paper ("Part 1") pointed out that, when $CO_2$ is injected at constant rate into a homogeneous 1-D flow system, the governing equations of the flow process have a similarity property: space and time dependence occurs only through a similarity variable $\zeta$, which for 1-D linear flow is given by $\zeta = x/t$, while for 1-D radial flow we have $\zeta = R^2/t$ (O'Sullivan, 1981). O'Sullivan showed that this remarkable property holds true even when all non-linearities of two-phase flow are taken into account, such as relative permeabilities and capillary pressures, and variations of fluid properties with thermodynamic conditions. It was shown in Part 1 that, as a consequence of the similarity property, solid saturation behind the dry-out front must be constant, independent of space and time. Numerical simulations presented in Part 1 have indeed confirmed this property. For 1-D displacement, the problem of determining solid precipitation behind the dry-out front is thus reduced to the problem of finding the single, constant value of $S_S$ behind the front.

In this section we will derive an analytical expression that allows to calculate $S_S$ directly from the properties of the fluids and the characteristics of the displacement process. This will be accomplished by considering mass conservation for water: water removed from the aqueous phase must equal water transferred into the $CO_2$ stream. We also invoke results from fractional flow theory (Buckley and Leverett, 1942) for the saturation profile established during the displacement process. The key physical process approximations made in the classical fractional flow theory include (i) treating fluids as incompressible, (ii) neglecting interphase mass transfer, and (iii) neglecting effects from capillary pressure. Recent work has extended fractional flow theory to account for interphase mass transfer (Johns, 1992; Dindoruk, 1992; Orr, 2007; Noh et al., 2007). However, mutual solubilities of $CO_2$ and $H_2O$ are small (a few percent) at typical temperature and pressure conditions of interest for $CO_2$ storage. As will be seen, the classical Buckley-Leverett theory, without allowance for interphase mass transfer effects on shock

propagation speeds, is sufficient to accurately account for precipitation effects from formation dry-out.

Injection of supercritical $CO_2$, henceforth for simplicity referred to as "gas," removes water from the vicinity of the injection point by two distinct mechanisms, (1) some water is immiscibly displaced by the advancing $CO_2$, and (2) some water is transferred (dissolved or evaporated) into the $CO_2$-rich gas phase. A displacement process without phase change would give rise to a Buckley-Leverett (1942) saturation profile, in which aqueous phase saturations cannot be reduced below the immobile liquid saturation $S_{lr}$. In contrast, dissolution into the gas phase can remove immobile water as well, and can lead to complete dry-out of the formation. Such effects have been observed in aquifer storage projects for natural gas (Lorenz and Müller, 2003). Specializing to 1-D linear flow, after some time t of $CO_2$ injection, dry-out will have advanced to a distance $x_d$ from the injection point. The amount of water that a displacement process without interphase mass transfer would leave behind in the region behind the dry-out distance $x_d$ is, per unit cross-sectional area of flow,[1]

$$M_{w,d} = \phi x_d \left(1 - \overline{S}_{g,d}\right) \rho_{aq} \left(1 - X_S - X_{CO2}\right) \quad (1)$$

where $\phi$ is porosity, $\overline{S}_{g,d}$ is the average gas phase saturation behind the dry-out front in the hypothetical displacement process without interphase mass transfer, $\rho_{aq}$ is aqueous phase density, and $X_S$ and $X_{CO2}$ are, respectively, the mass fractions of salt and $CO_2$ dissolved in the aqueous phase. The water mass given by Eq. (1) has been removed from the dry-out region by uptake into the flowing $CO_2$ stream. We now consider the amount of water present in the gas phase per unit cross-sectional flow area, which is given by

$$M_{w,g} = \phi \left(x_f - x_d\right) \overline{S}_{g,fd} \rho_g Y_g \quad (2)$$

[1] This and the following equations apply to 1-D radial flow as well, employing the substitution x ==> $\pi R^2$ to normalize per unit formation thickness.

Eq. (2) expresses the fact that the $CO_2$ in the dry-out region contains no water, while water is present in the gas phase in the two-phase zone $x_d \le x \le x_f$ . $\overline{S}_{g,fd}$ is the average gas saturation in the two-phase region, $\rho_g$ is gas density, and $Y_g$ is equilibrium mass fraction of water in the gas phase at prevailing conditions of temperature, pressure, and salinity (Spycher and Pruess, 2005). Water in the gas phase originates from two different sources, namely, from the dry-out region and from the aqueous phase in the two-phase zone. As gas phase flows outward in the two-phase zone, its pressure and density are becoming smaller. This will reduce the water mass fraction in the gas phase, and induce some additional water uptake by the $CO_2$-rich phase in the two-phase zone. However, for typical $CO_2$ injection conditions of interest, the additional water uptake into the gas phase from depressurization, as well as due to the lower salinity in the two-phase zone, is negligibly small relative to the water uptake at the dry-out front (Pruess and Spycher, 2007). Accordingly, we assert that the amount of water present in the gas phase is equal to the amount removed from the dry-out region, i.e., $M_{w,g} = M_{w,d}$, so that from Eqs. (1, 2) we have

$$x_d\left(1-\overline{S}_{g,d}\right) \;=\; \left(x_f - x_d\right)\overline{S}_{g,fd}\,F \tag{3}$$

Here we have collected relevant fluid properties in the coefficient F, given by

$$F \;=\; \frac{\rho_g Y_g}{\rho_{aq}\left(1-X_S-X_{CO2}\right)} \tag{4}$$

Eq. (3) with the definition Eq. (4) establishes a relationship between fluid properties and frontal parameters and saturations of the displacement process. For conditions of interest to $CO_2$ storage, $\rho_g < \rho_{aq}$ and $F < Y_g$; $Y_g$ typically is on the order of 0.5 % or less (Spycher and Pruess, 2005), so that $F < 5x10^{-3}$. To proceed further, we need to relate saturations in different portions of the displacement profile. From the definition of averages we have

$$x_f\overline{S}_g \;=\; x_d\overline{S}_{g,d} + \left(x_f - x_d\right)\overline{S}_{g,fd} \tag{5}$$

where $\overline{S}_g$ is the average gas saturation behind the two-phase front. Solving Eq. (5) for $(x_f - x_d)\overline{S}_{g,fd}$, inserting into the r.h.s. of Eq. (3) and rearranging we obtain

$$x_d\left(1-\overline{S}_{g,d}\left[1-F\right]\right) \quad = \quad x_f\overline{S}_g F \tag{6}$$

As had been mentioned, for typical temperature and pressure conditions of interest in geologic storage of $CO_2$, the parameter group F is small, of order $5x10^{-3}$ or less. Accordingly, F may be neglected in comparison to 1 on the l.h.s. of Eq. (6), and we have

$$x_d\left(1-\overline{S}_{g,d}\right) \quad = \quad x_f\overline{S}_g F \tag{7}$$

Further, from standard fractional flow theory, we have (see Appendix)

$$x_d\overline{S}_{g,d} \quad = \quad x_d S_{g,d} + x_f\overline{S}_g\left(1-f_d\right) \tag{8}$$

and

$$\frac{x_d}{x_f} \quad = \quad \left.\frac{df}{dS}\right|_{S_{g,d}} \overline{S}_g \tag{9}$$

where $f_d$ is the fractional flow of gas phase at saturation $S_{g,d}$ at the dry-out front, and $\left(df/dS\right)_{S_{g,d}}$ is the derivative of fractional flow of gas at the dry-out front. Note that dependence on relative permeabilities arises only through the fractional flow function (Eq. A.1) and its derivative. Using Eqs. (8, 9) in Eq. (7) and dividing by $x_f\overline{S}_g$ we obtain

$$\left(1-S_{g,d}\right)\left.\frac{df}{dS}\right|_{S_{g,d}} + f_d - 1 \quad = \quad F \tag{10}$$

For given values of aqueous and gas viscosities, the l.h.s. of Eq. (10) is a non-linear function of $S_{g,d}$, the gas saturation at the dry-out front,

$$G\left(S_{g,d}\right) = \left(1-S_{g,d}\right)\left.\frac{df}{dS}\right|_{S_{g,d}} + f_d - 1 \tag{11}$$

while the fluid property coefficient F on the r.h.s. is a function of thermodynamic conditions (temperature, pressure, salinity and $CO_2$ concentration of the aqueous phase; see Eq. 4). For given relative permeabilities and fluid properties (phase densities and viscosities, mass fraction of water in gas and salt in the aqueous phase), Eq. (10) is an implicit equation for the gas saturation at the dry-out front $S_{g,d}$ that may be solved by iteration. Alternatively, $S_{g,d}$ may be found analytically from fractional flow theory (Noh et al., 2007). Having found $S_{g,d}$, Eqs. (8, 9) can then be used to obtain the average gas saturation $\overline{S}_{g,d}$ in the region behind the dry-out front as follows

$$\overline{S}_{g,d} = S_{g,d} + \frac{x_f}{x_d}\overline{S}_g\left(1-f_d\right) = S_{g,d} + \frac{1-f_d}{\left(df/dS\right)_{S_{g,d}}} \tag{12}$$

The salt inventory in the aqueous phase that would be left behind in the region $0 \le x \le x_d$ in a hypothetical displacement without interphase mass transfer is

$$M_S = x_d\phi\left(1-\overline{S}_{g,d}\right)\rho_{aq}X_S \tag{13}$$

Dividing by the solid mass that would be needed to fill the entire pore space in the dry-out zone, the single value of solid saturation corresponding to this salt inventory can then be obtained as

$$S_S = \frac{M_S}{x_d\phi\rho_S} = \left(1-\overline{S}_{g,d}\right)\frac{\rho_{aq}X_s}{\rho_s} \tag{14}$$

Accordingly, the procedure for estimating solid saturation $S_S$ involves three steps, (1) obtain gas saturation $S_{g,d}$ at the dry-out front, either by iteratively solving Eq. (10), or directly from

fractional flow theory (Noh et al., 2007), (2) use $S_{g,d}$ and the fractional flow function in Eq. (12) to calculate average gas saturation $\overline{S}_{g,d}$ in the dry-out region, and (3) use Eq. (14) to obtain solid saturation $S_S$.

We note that standard fractional flow theory also provides an estimate for the advancement of the dry-out front; it advances with constant speed and its location at time t is (see Appendix)

$$x_d = t \frac{u}{\phi} \frac{df}{dS}\bigg|_{S_{g,d}} \tag{15}$$

where u is the volumetric rate of injection per unit cross-sectional area.

All derivations given above are valid for 1-D radial flow as well, making the substitutions $x \Longrightarrow \pi R^2$, and interpreting u as volumetric injection rate per unit formation thickness.

**3. Discussion and Examples.**

From Eqs. (10, 12, 14) it is apparent that the solid saturation predicted by the analytical model does not depend on formation porosity. This was checked and confirmed by running full numerical simulations of the $CO_2$ injection process (see Table 2 of Part 1, Case 7). In the fractional flow approximation, the saturation profile is independent of injection rate. In the analytical model of Sec. 2, a dependence of $S_S$ on injection rate would arise only because some of the fluid properties in F (Eq. 4) are pressure sensitive, and different injection rates will affect overall pressurization.

The calculation of solid saturations from Eqs. (10, 12, 14) poses no difficulties. The l.h.s of Eq. (10) is a smoothly-varying function that ranges over many orders of magnitude when gas saturation is varied (Fig. 2). Parameters used for calculating fractional flow and the saturation function $G(S_{g,d})$ of Eq. (11) are given in Table 1. The fluid parameter F is calculated from correlations expressing fluid density and $CO_2$-brine phase partitioning as function of temperature, pressure, and salinity (Spycher and Pruess, 2005). The example portrayed in Fig. 2

involves $CO_2$ injection into a 1-D radial system with initial conditions of (T, P, $X_S$) = (50 ºC, 120 bar, 25 %), for which the relevant parameters as obtained by a full numerical simulation in Part 1 are $\rho_g$ = 710 kg/m$^3$, $\rho_l$ = 1180 kg/m$^3$, $Y_g = 0.224 \times 10^{-2}$, $X_S = 0.246$, $X_{CO2} = 1.57 \times 10^{-2}$, yielding $F = 1.826 \times 10^{-3}$. Eq. (10) is solved by tabulating $G(S_g)$ in decrements of $\Delta S_g = 0.01$, starting from the largest possible gas saturation, $S_{g,max}=1-S_{lr}$. We monitor G as $S_g$ is decremented and, when G increases beyond F, we perform linear interpolation over the interval with $G_1 < F < G_2 = G_1 + 0.01$ to find $S_{g,d}$ such that $G(S_{g,d}) = F$.

To obtain the average gas saturation $\overline{S}_{g,d}$ in the dry-out region from $S_{g,d}$, we apply the same linear interpolation as for $S_{g,d}$ to the last term on the r.h.s of Eq. (12), (1-f)/(df/dS). The resulting value of $\overline{S}_{g,d}$ is then inserted in Eq. (14) to obtain solid saturation.

<Fig. 2 here>

The approximately exponential dependence of G on $S_g$ makes the saturation solution of Eq. (10) robust and insensitive to modest variations in F. Gas phase density enters F as a coefficient (Eq. 4), and can vary significantly, by as much as a factor 2, depending on fluid pressures during $CO_2$ injection. (Additional, smaller pressure sensitivity arises also from the dependence of $CO_2$ viscosity on pressure.) For testing the accuracy of the analytical model by comparing with results of numerical simulations, we can use fluid properties from the simulation that account for pressurization effects. However, if the analytical model is to be a useful tool for obtaining a simple, approximate estimate of $S_S$, we need to be able to apply it without having information from a numerical simulation available. As will be seen below, the estimation of frontal saturation from Eq. (10) is sufficiently insensitive to variations in F that using $CO_2$ density at original *in situ* temperature and pressure conditions, without allowance for pressurization effects on gas density, will provide satisfactory accuracy for determining $S_{g,d}$.

The analytical model derived in Section 2 was applied to evaluate solid saturations for a range of formation and fluid parameters. Most calculations were done for brine properties as in Part 1, namely, T = 50 ºC, P = 120 bar, Xs = 0.25; and using the same relative permeability functions (van Genuchten, 1980; Corey, 1954). Table 1 compares predictions from our analytical

theory for $S_S$ with results from numerical simulations, listing two estimates from the analytical theory, one for fluid properties corresponding to initial conditions ("@INCON"), another for fluid properties corresponding to the average simulated pressures in the two-phase zone ("@ P"). The analytical estimates for $S_S$ are seen to agree very closely with the numerical results, usually within a relative error of less than 1 %.

<Table 1 here>

The results shown in Table 1 indicate a strong dependence of solid saturation $S_S$ on aqueous phase salinity, as expected. $S_S$ also depends strongly on multiphase flow parameters (relative permeability), but dependence on temperature and pressure is weak. This may seem surprising in view of the fact that the function F of fluid properties (Eq. 4) has a significant dependence on temperature and pressure, through the parameter group $\rho_g Y_g$ in the numerator. The explanation for the limited sensitivity to T, P is that gas phase viscosity $\mu_g$ generally also increases when $\rho_g Y_g$ increases, which compensates for the effects on F. In particular, predictions for $S_S$ with using initial aquifer pressures agree very closely with predictions that take into account increased fluid pressures from injection, as obtained from the numerical simulations. This insensitivity to fluid pressures makes it possible to get accurate estimates for $S_S$ on the basis of initial thermodynamic conditions, and makes the analytical model useful for direct estimation of $S_S$ from multiphase flow parameters and in situ fluid properties, without having to perform numerical simulations.

**4. Concluding Remarks.**

Injection of dry $CO_2$ into a saline aquifer will lead to water being displaced immiscibly, as well as being transferred (dissolved or evaporated) into the supercritical $CO_2$ phase. Interphase mass transfer of water may lead to formation dry-out, accompanied by precipitation of solid salts that will reduce formation porosity, permeability, and injectivity.

This paper has presented a simple analytical model for $CO_2$ injection at constant rate into a homogeneous medium in 1-D linear or radial flow geometry. Under such conditions the problem has a similarity property, even when accounting for all of the non-linearities involved in

multiphase flow. From the similarity property it follows that solid precipitation due to dry-out will generate a constant solid saturation (= fraction of pore space containing precipitate) behind the dry-out front. By considering a mass balance for water transferred by dry-out into the $CO_2$-rich phase, we have been able to derive analytical expressions for the solid saturation as implicit function of fluid properties (densities, compositions, viscosities) and parameters of the displacement process (relative permeabilities). Comparison with detailed numerical simulations demonstrated that our simple analytical model is able to predict solid precipitation with excellent accuracy.

**Appendix: Some Results from Fractional Flow Theory**

Fractional flow theory (Buckley and Leverett, 1942; Willhite, 1986; Binning and Celia, 1999) considers the Darcy flow of two immiscible fluids (e.g. oil and water, or water and gas) through a homogeneous porous medium, neglecting effects of fluid compressibility, capillary pressure, and interphase mass transfer. With these approximations, the fundamental mass conservation equations for the two fluids reduce to purely hyperbolic form, and give rise to traveling saturation profiles with self-sharpening saturation shocks (discontinuities). Saturation profiles are determined by relative permeabilities $k_{rg}$, $k_{rl}$ and viscosities $\mu_g$, $\mu_l$ of the two phases through the "fractional flow function" f, given by

$$f_g(S_g) = \frac{k_{rg}/\mu_g}{k_{rg}/\mu_g + k_{rl}/\mu_l} \qquad (A.1)$$

Here we have written the fractional flow function $f_g$ for gas; an analogous equation holds for the liquid phase function $f_l = 1 - f_g$. The fractional flow depends upon saturation $S_g$ (or $S_l = 1 - S_g$) in a generally extremely non-linear fashion, through the relative permeability functions $k_{rg}(S_g)$ and $k_{rl}(S_l)$. For conditions of interest in the $CO_2$-brine system, liquid (brine) viscosity may exceed that of the gas phase by factors of order 10 or more; this viscosity contrast will favor gas flow.

Due to the incompressibility assumption, total volumetric flow rate of the two phases is constant throughout, independent of position. The physical significance of the fractional flow function is that it represents the volume fraction of each phase in the total flow. From the fractional flow function, all aspects of the flow dynamics can be derived, such as frontal saturation, saturation profiles, and the relationship between frontal saturation and saturation average behind the front (Buckley and Leverett, 1942; Welge, 1952).

Consider a displacement profile as schematically shown in Fig. 1, and calculate the gas-filled pore volume $V_d$ out to some distance $x_d$, behind the displacement front at $x_f$. For 1-D linear flow in a homogeneous porous medium with unit cross-sectional flow area, we have (see Fig. 1)[2]

[2] This and the following equations apply to 1-D radial flow as well, employing the substitution x ==> $\pi R^2$ to normalize per unit formation thickness.

$$V_d = \phi \int_0^{x_d} S_g dx = \phi S_{g,d} x_d + \phi \int_{S_{g,d}}^{S_{g,0}} x dS \tag{A.2}$$

The speed of propagation of a gas saturation S is proportional to the volumetric rate of injection u and the derivative of the fractional flow function, df/dS,

$$\frac{dx}{dt} = \frac{u}{\phi}\frac{df}{dS} \tag{A.3}$$

Integrating (A.3) with respect to x and t, the propagation distance of saturation S is

$$x = \frac{u}{\phi}\frac{df}{dS}t \tag{A.4}$$

Inserting Eq. (A.4) into the integral on the r.h.s. of Eq. (A.2), we have

$$V_d = \phi S_{g,d} x_d + ut\left(1 - f_d\right) \tag{A.5}$$

Expressing $V_d$ in terms of average gas saturation $\overline{S}_{g,d}$ in the region $0 \le x \le x_d$, $V_d = \phi \overline{S}_{g,d} x_d$, we obtain

$$\phi \overline{S}_{g,d} x_d = \phi S_{g,d} x_d + ut\left(1 - f_d\right) \tag{A.6}$$

By writing the total injected volume ut in terms of the average gas saturation $\overline{S}_g$ behind the displacement front $x_f$, $ut = \phi \overline{S}_g x_f$, we obtain Eq. (8).

From Eq. (A.4) we can obtain a relationship between the propagation distances for two different saturations, $S_d$ and $S_f$, as follows.

$$\frac{x_d}{x_f} = \frac{(df/dS)_{S_d}}{(df/dS)_{S_f}} \tag{A.7}$$

At the displacement front we have (Welge, 1952)

$$\left.\frac{df}{dS}\right|_{S_f} = \frac{f(S_f)}{S_f} = \frac{1}{\bar{S}_g} \tag{A.8}$$

Inserting Eq. (A.8) into (A.7) we obtain Eq. (9).

**Acknowledgement**

Thanks are due to Yu-Shu Wu for a careful review of the manuscript and the suggestion of improvements. I also thank Jan Nordbotten and three anonymous reviewers for valuable suggestions that have improved the paper. This work was supported by the Zero Emission Research and Technology project (ZERT) under Contract No. DE-AC02-05CH11231 with the U.S. Department of Energy.

**References**

Binning, P. and M.A. Celia. Practical implementation of the fractional flow approach to multi-phase flow simulation, *Adv. Wat. Resour.,* Vol. 22, No. 5, pp. 461–478, 1999.

Buckley, S.E. and M.C. Leverett. Mechanism of Fluid Displacement in Sands, *Trans. Am. Inst. Min. Metall. Eng.,* Vol. 146, pp. 107 - 116, 1942.

Corey, A.T. The Interrelation Between Gas and Oil Relative Permeabilities, *Producers Monthly*, pp. 38 - 41, November 1954.

Dindoruk, B. Analytical Theory of Multicomponent Displacement in Porous Media, PhD thesis, Stanford University, Stanford, CA, 1992.

Johns, R.T. Analytical Theory of Multiphase Multicomponent Gas Drives with Two-Phase Mass Transfer, PhD thesis, Stanford University, Stanford, CA, 1992.

Lorenz, S. and W. Müller. Modelling of Halite Formation in Natural Gas Storage Aquifers, *Proceedings, TOUGH Symposium 2003,* Lawrence Berkeley National Laboratory, Berkeley, CA, May 2003.

Noh, M., L.W. Lake, S.L. Bryant and A. Araque-Martinez. Implications of Coupling Fractional Flow and Geochemistry for CO2 Injection in Aquifers, *SPE Reservoir Evaluation and Engineering,* pp. 406–414, August 2007.

Nordbotten, J.M. and M.A. Celia. Similarity Solutions for Fluid Injection into Confined Aquifers, *J. Fluid Mech.,* Vol. 561, pp. 307–327, 2006.

Orr Jr., F.M. *Theory of Gas Injection Processes,* Tie-Line Publications, Copenhagen, Denmark, 2007.

O'Sullivan, M.J. A Similarity Method for Geothermal Well Test Analysis, *Water Resour. Res.*, Vol. 17, No. 2, pp. 390 – 398, 1981.

Pruess, K. The TOUGH Codes—A Family of Simulation Tools for Multiphase Flow and Transport Processes in Permeable Media, *Vadose Zone J.,* Vol. 3, pp. 738 - 746, 2004.

Pruess K. and N. Spycher. ECO2N – A Fluid Property Module for the TOUGH2 Code for Studies of CO2 Storage in Saline Aquifers, *Energy Conversion and Management,* Vol. 48, No. 6, pp. 1761–1767, doi:10.1016/j.enconman.2007.01.016, 2007.

Spycher, N. and K. Pruess. $CO_2$-$H_2O$ Mixtures in the Geological Sequestration of $CO_2$. II. Partitioning in Chloride Brines at 12–100 °C and up to 600 bar, *Geochim. Cosmochim. Acta,* Vol. 69, No. 13, pp. 3309–3320, doi:10.1016/j.gca.2005.01.015, 2005.

van Genuchten, M.Th. A Closed-Form Equation for Predicting the Hydraulic Conductivity of Unsaturated Soils, *Soil Sci. Soc. Am. J.*, Vol. 44, pp. 892 - 898, 1980.

Welge, H.J. A Simplified Method for Computing Oil Recoveries by Gas or Water Drive, *Trans.,* AIME, Vol. 195, pp. 91 - 98, 1952.

Willhite, G.P. *Waterflooding,* Society of Petroleum Engineers, Richardson, TX, 1986.

Tables

Table 1. Predictions of solid saturations for a variety of porous media.

| Case | Correspondence to Part 1 | k ($m^2$) | $S_{lr}$ | m | $S_S$ analytical @INCON | $S_S$ analytical @ P | $S_S$ numerical |
|---|---|---|---|---|---|---|---|
| A | Case 2 | 100.e-15 | .30 | .457 | 6.69 % | 6.70 % | 6.72 % |
| B | Case 2 but $X_s = 0.125$ | 100.e-15 | .30 | .457 | 3.00 % | 3.00 % | 2.97 % |
| C | as Case 2, but different $k_{rl}$ | 3.64e-13 | .256 | .3243 | 7.46 % | 7.46 % | 7.48 % |
| D | as Case 2, but $k_{rl}$ from Part 1, Sec. 2 | 33.3e-15 | .263 | .1870 | 9.17 % | 9.26 % | 9.15 % |
| E | as Case 2, but T = 30 ºC | 100.e-15 | .30 | .457 | 6.65 % | 6.65 % | 6.62 % |
| F | as Case 2, but P = 200 bar | 100.e-15 | .30 | .457 | 6.74 % | 6.74 % | 6.73 % |

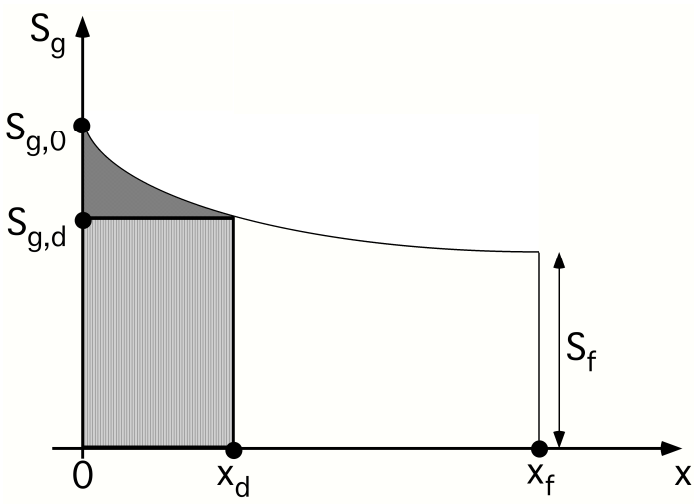


Figure 1. Schematic of saturation profile for supercritical CO2 displacing brine. The injection point is at x = 0, the dry-out region with salt precipitation extends to $x_d$, and the two-phase front is at $x_f$. Regions with different shading relate to evaluation of the integral in Eq. (A.2).

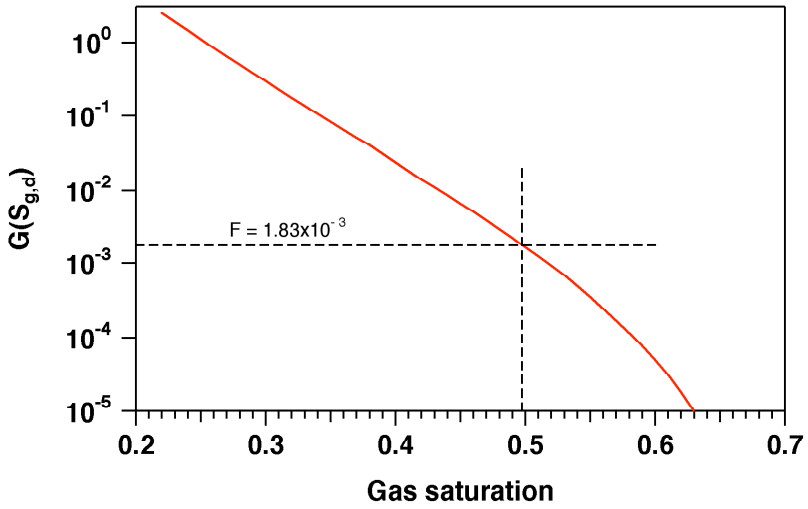


Figure 2. The l.h.s. of Eq. (10) plotted as a function of gas saturation for properties corresponding to Case A in Table 1. Saturation at the dry-out front is given by the intercept with $F = 1.83 \times 10^{-3}$, and is $S_{g,d} = 49.7$ %.